entations for a triangle or a pentagon with ensuing $\mathbf{n}(\mathbf{r})$ having at least two planes of mirror symmetry: (i) one with a side along $\mathbf{n}_0$ giving an

Supporting Online Material

Shape Controlled Colloidal Interactions in Nematic Liquid Crystals

Clayton P. Lapointe[1,2], Thomas G. Mason[2], and Ivan I. Smalyukh[1,1]

1

8 developer s

calculated in real time and relayed to the spatial

and strength of surface anchoring. The symmetry of **n**(**r**) does not change when either surface anchoring or size of an odd-*N* platelet such as a triangle is reduced (Figs. S1D and E); the deformations are smaller, and therefore, the magnitude of **p** is smaller than in the strong anchoring case, but the **n**(**r**) structure remains dipolar. This behavior is similar to the case of spherical colloids with planar surface anchoring retaining their quadrupolar symmetry of **n**(**r**) with varying the particle size and anchoring strength (Figs. S1J and K).

The above differences between the behavior of spherical and anisotropic colloids can be understood by considering the bulk elastic and surface anchoring energy associated with introducing the colloidal inclusions into the NLC. The Frank elastic energy of NLCs can be expressed in terms of spatial gradients of **n**(**r**):

(S1)

where K_{11}, K_{22}, and K_{33} are three independent Frank elastic constants corresponding to !splay", !bend", and !twist" deformations respectively (*S18*) and the integration is carried out over the volume of the NLC. The three elastic constants of thermotropic small molecule nematics are of the same order of magnitude [e.g. for 5CB at room temperature K_{11} å 6.4 pN, K_{22} å 3 pN, and K_{33} å 10 pN (*S19*)]. In the one elastic constant approximation, Eq. (S1) is often approximated as

Particle displacements along and perpendicular to $\mathbf{n_0}$ (x and y, respectively) over various delay times were extracted from the trajectory data shown in Fig. S3A. Histograms sampled from the time-delayed displacements are well described by Gaussian distributions with different widths or mean-square displacements, $^{2}_{\|,}$ (Fig. S3B). As is shown in Fig. S3C, the two mean-square

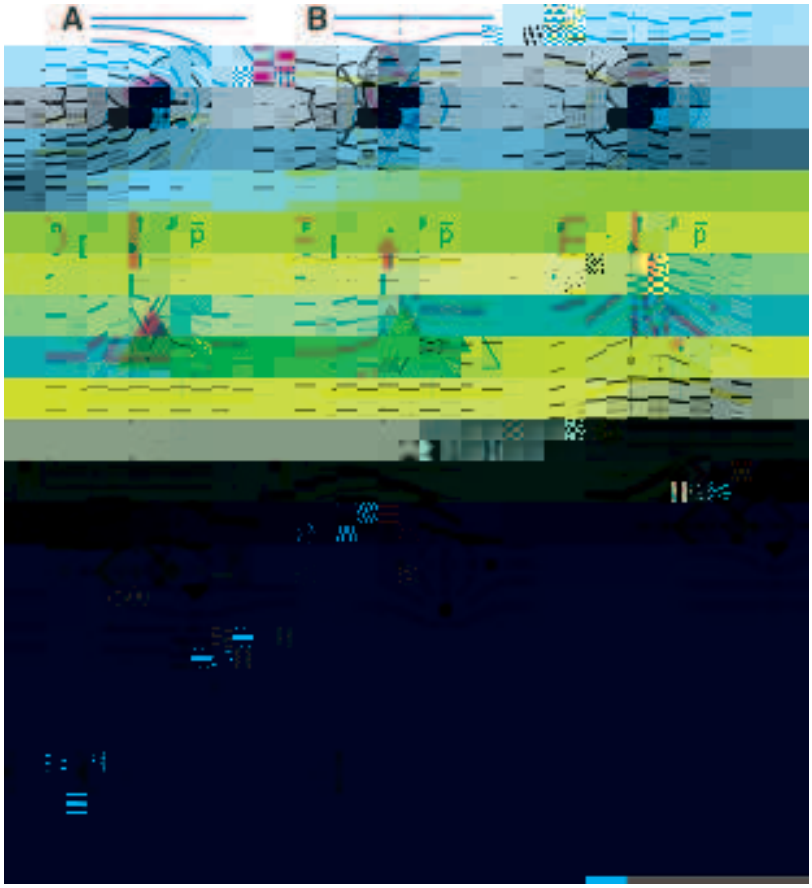

Fig. S1. Effects of surface anchoring and particle size on the symmetry of director structures induced by colloids. For spheres with vertical surface anchoring, reducing their size or weakening the surface anchoring changes the symmetry of **n**

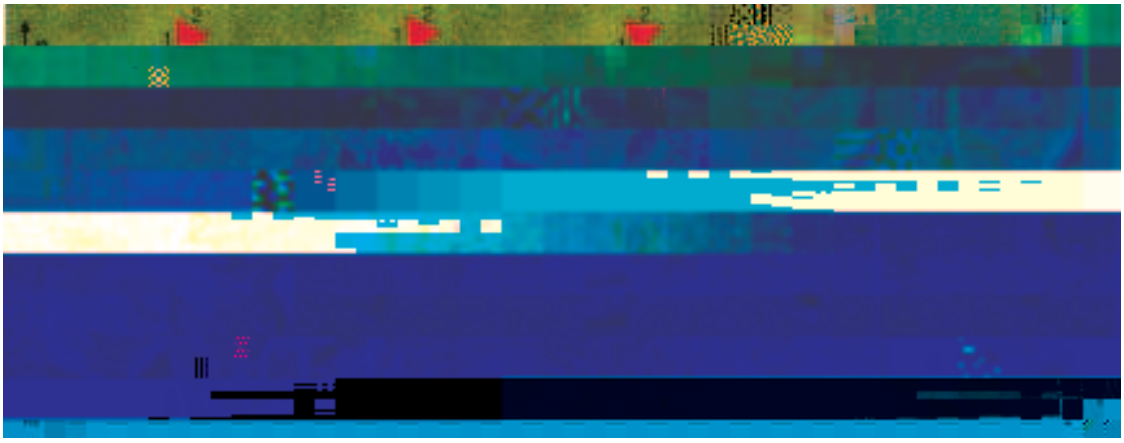

Fig. S3. Drag coefficients of a colloidal square in 5CB via diffusion measurements. (**A**) Blue points show the trajectory of the square in the background image determined from a video of total duration 1000 sec acquired at a frame rate of 15 Hz. The double-headed arrow shows the far-field alignment direction $\mathbf{n}_0$. (**B**) Histograms for displacements along the x-direction (circles) and the y-direction (squares) extracted from the trajectory data in (A) with sampling time delays of =0.33 sec (top) and =1.5 sec (bottom). Black lines show Gaussian fits to the histograms. (**C**) Mean square displacement ^{2} parallel to $\mathbf{n}_0$ (circles) and ^{2} perpendicular to $\mathbf{n}_0$ (squares) as a function of . Slopes determined with linear fits to the data give values of the two diffusion

SOM REFERENCES

(*S1*) C. J. Hernandez, T. G. Mason, *J. Phys. Chem. C* **111**, 4474 (2007).

(*S2*) A. Ashkin, *Proc. Natl. Acad. Sci.* **94**, 4853 (1997).

(*S3*) Z. Cheng, P. M. Chaikin, T. G. Mason, *Phys. Rev. Lett.* **89**, 108303 (2002).

(*S4*) I. I. Smalyukh, S. V. Shiyanovskii, O. D. Lavrentovich, *Chem. Phys. Lett.* **336**, 88 (2001).

(*S5*) O. Mondain-Monval, J. C. Dedieu, T. Gulik-Krzywicki, P. Poulin, *Eur. Phys. J. B* **12**, 167 (1999).

(*S6*) K. Kita, M. Ichikawa, Y. Kimura, *Phys. Rev. E* **77**, 041702 (2008).

(*S7*) H. Stark, *Eur. Phys. J. B* **10**, 311 (1999).

(S8) D. Andrienko, G. Germano, M. P. Allen, *Phys. Rev. E* **63**, 041701 (2001).

(*S9*) O. Guzmán, E. B. Kim, S. Grollau, 0.535201Cl